

Ab initio theory of Cr_2O_3 surface chemistry in solution

S. Petrosyan and T.A. Arias

Department of Physics, Cornell University, Ithaca, NY 14853

A.A. Rigos

Department of Chemistry, Merrimack College, North Andover, MA

Using a new form of density functional theory for the *ab initio* description of electronic systems in contact with a dielectric environment, we present the first detailed study of the impact of a solvent on the surface chemistry of Cr_2O_3 , the passivating layer of stainless steel alloys. Compared to vacuum, we predict that the presence of water has little impact on the adsorption of chloride ions to the oxygen-terminated surface but a dramatic effect on the binding of hydrogen to that surface. These results indicate that the dielectric screening properties of water are important to the passivating effects of the oxygen-terminated surface.

1. INTRODUCTION

Ab initio calculations have shed light on many physico-chemical questions, including chemical reactions in solution and chemical reactions at surfaces [1, 2, 3]. Although computational chemistry is now able to provide not only qualitative but also quantitative insights into surface chemistry [2], so far these studies have been limited to reactions in a vacuum even though experimentally these reactions often occur in a solvent environment.

Each year, corrosion costs the United States \$276 billion [4], approximately 3.1% of the gross domestic product, and many approaches have been used to understand and model this complex process [5, 6, 7]. High performance stainless steel alloys contain chromium to result in the formation of a Cr_2O_3 passivating surface layer, which provides corrosion resistance. Even with this layer, such alloys are susceptible to breakdown in acidic, chlorine-containing aqueous environments[8, 9], the study of which demands simultaneous treatment of surfaces, reactants and the aqueous dielectric environment. Direct experiments are difficult, and although *ab initio* calculations have a history of answering many such questions, to date they have not been able to address the effect of the solvent on surface reactions. Alavi *et al.*[10], for instance, have studied the adsorption of HCl on single-crystal $\alpha\text{-Al}_2\text{O}_3$ (0001) surfaces and calculated adsorption energies as a function of surface coverage within density-functional theory, but all of their results are obtained in a vacuum environment.

Previous studies of Cr_2O_3 have been limited to pure surfaces in vacuum [11], an unrealistic environment for the study of corrosion. These studies indicated that the highest occupied and lowest unoccupied molecular orbitals are localized on the chromium ions, suggesting that the oxygen-terminated surface could provide a stable barrier against acidic chlorinated environments *if* the surface oxygen layer could be prevented from reacting with species in the solution. The work below puts forth evidence to support the novel hypothesis that the dielectric screening effects associated with an aqueous environment actually prevent the formation of bonds with aqueous species such as protons, thereby rendering the

oxygen-terminated surface virtually non-reactive.

Models for calculating solvation energies from continuum dielectric theory[12] have been applied to single molecules or activated complexes but not to molecules adsorbed on surfaces, perhaps because such methods are generally applied to molecules. Here, we introduce the first approach to *ab initio* calculations in a dielectric environment which sits on a firm theoretical foundation. Below, we show that this new approach, which in a simple approximation is related to that recently introduced by Fattebert and Gygi[13], gives results in good agreement with currently accepted quantum chemical methods and is well-suited to surfaces. Finally, we apply the approach to carry out the first *ab initio* study of the reactivity of hydrogen and chlorine on an oxygen-terminated Cr_2O_3 (0001) surface in contact with a solution.

2. THEORETICAL APPROACH

Because of the large cells required in this study (well over one hundred atoms), the only practicable *ab initio* approach suited to describe the electrons of the surface and the reactants is density-functional theory[11]. The periodicity of the surface makes periodic boundary conditions and thus the plane-wave pseudopotential method [14] the most natural choice. The size of the surface cell and time-scales needed for proper thermodynamic averaging make a direct molecular dynamics treatment of the aqueous environment infeasible, thus raising the question of how to treat the solvent. This work takes the novel approach of exploiting the existence of so-called “classical” density-functional theories[15], which can treat water rigorously in terms of a simple thermodynamically averaged molecular density and an approximate functional[16]. We then introduce here for the first time the concept of a *joint density-functional theory* (JDFT) between the electrons in the surface and the molecules comprising the solvent.

In a companion to this paper[17], we prove that the total thermodynamic free energy A of an electronic system (solute) with nuclei of charges Z_I at locations R_I in equilibrium with a closed-shell liquid molecular environ-

ment (solvent) may be determined from the variational principle

$$A = \min_{n(r), N(r)} (A_{KS}[n(r), \{Z_I, R_I\}] + A_{Iq}[N(r)] + U[n(r), N(r), \{Z_I, R_I\}]), \quad (1)$$

where, at the minimum, $n(r)$ is the thermo- and quantum- mechanically averaged density of the electrons of the solute and $N(r)$ is the likewise averaged molecular density of the solvent. $A_{KS}[n(r), \{Z_I, R_I\}]$, $A_{Iq}[N(r)]$ and $U[n(r), N(r), \{Z_I, R_I\}]$ appearing above are, respectively, the standard Kohn-Sham electron-density functional of the solute when in isolation, the classical density-functional for the molecular solvent when in isolation, and a new functional describing the coupling between the systems. The new functional $U[n(r), N(r), \{Z_I, R_I\}]$ is universal in the sense that it depends only upon the nature of the solvent and is independent of the nature of the solute. For completeness, we note that each of the three aforementioned functionals is implicitly also a function of the temperature T .

In the present work, we make the further simplification of performing the minimization over $N(r)$ in (1), resulting in the variational principle

$$A = \min_{n(r)} (A_{KS}[n(r), \{Z_I, R_I\}] + W[n(r), \{Z_I, R_I\}]), \quad (2)$$

where

$$W[n(r), \{Z_I, R_I\}] \equiv \min_{N(r)} (A_{Iq}[N(r)] + U[n(r), N(r), \{Z_I, R_I\}])$$

is a universal functional dependent solely upon the identity of the environment (and, implicitly, the temperature). Note that, in principle, the theory at this stage is exact. Below we outline the approximations which we introduce because the exact form of the functionals $A_{KS}[n(r), \{Z_I, R_I\}]$ and $W[n(r), \{Z_I, R_I\}]$ are unknown.

3. COMPUTATIONAL DETAILS

For treatment of the electrons in the chromium-oxide surface through the functional $A_{KS}[n(r), \{Z_I, R_I\}]$, we apply the standard local spin-density approximation (LSDA)[18]. The calculations themselves employ the total-energy plane-wave density-functional pseudopotential approach [14] with potentials of the Kleinman-Bylander form [19] with p and d non-local corrections at a cutoff of 40 hartrees. Supercells with periodic boundary conditions in all three dimensions represent the surfaces of isolated oxygen-terminated (0001)-oriented slabs of Cr_2O_3 of thickness 13 Å separated by 7.8 Å of either vacuum or solvent. The in-plane boundary conditions suffice to describe 2×2 reconstructions and consist of four times the unit from [11] so as to allow sufficient isolation of solvent volumes excluded by chlorine adsorbed on the

surface. The supercell contains a total of forty chromium and seventy-two oxygen atoms with chlorine or hydrogen added to the two surfaces in inversion-symmetric pairs, one on each side of the slab. Finally, we use a single k -point to sample the Brillouin zone of the surface slab. Ref. [11] establishes that this choice of functional, pseudopotential, plane-wave cutoff, sampling density in the Brillouin zone and supercell gives a good description of the bulk and surface of Cr_2O_3 . As in the aforementioned work, we employ the analytically continued functional approach [14, 20] to minimize the Kohn-Sham energy with respect to the electronic degrees of freedom. Below, we relax all ionic configurations until the total energy is within 0.027 eV of the minimum and the maximum force in any direction is less than 0.3 eV/Å.

For the environment functional $W[n(r), \{Z_I, R_I\}]$ in (2), we take the interaction of the electron and nuclear charges of the system under study with a dielectric environment in which the dielectric constant is local in space and has a value dependent only upon the electron density at each point, $\epsilon(r) \equiv \epsilon(n(r))$. In practice, we compute the total free energy of the system in contact with the environment by finding the stationary point with respect to both the electrons and the mean electrostatic field $\phi(r)$ of the functional

$$A = A_{TXC}[n_\uparrow(r), n_\downarrow(r)] + \Delta V_{ps}[n_\uparrow(r), n_\downarrow(r)] + \int d^3r \left\{ \phi(r) \left(n_{tot}(r) - \sum_I Z_I \delta^{(3)}(r - R_I) \right) - \frac{\epsilon(n(r))}{8\pi} |\nabla \phi(r)|^2 \right\} \quad (3)$$

where $n_\uparrow(r)$, $n_\downarrow(r)$ and $n_{tot}(r)$, respectively, are the up-, down- and total electron densities, $A_{TXC}[n_\uparrow(r), n_\downarrow(r)]$ is the Kohn-Sham single-particle kinetic plus exchange correlation energy within the local spin-density approximation, ΔV_{ps} is the difference in the total pseudopotential energy from that expected from pure Coulomb interactions with point ions of valence charges Z_I at locations R_I , and $\delta^{(3)}(r)$ is the three-dimensional Dirac- δ function. Note that, although we do work directly with the Kohn-Sham orbitals, for brevity we have written the above in terms of the electron densities. We also note that at this level of approximation our joint density functional theory takes the same form as the approach of [13], which introduced the form as a computational device without formal justification or proof.

For the local dielectric function $\epsilon(n(r))$, we choose a specific form which varies smoothly from the dielectric constant of the bulk solvent ϵ_b when the electron density $n(r)$ is less than a critical value n_c indicative of the interior of the solvent to the dielectric constant of vacuum $\epsilon = 1$ when $n(r) > n_c$. Specifically, we take

$$\epsilon(n) = 1 + \frac{\epsilon_b - 1}{2} \operatorname{erfc} \left(\frac{\ln(n/n_c)}{\sqrt{2}\sigma} \right), \quad (4)$$

where the parameter σ , to which the results are not very sensitive, controls the width of the transition from bulk

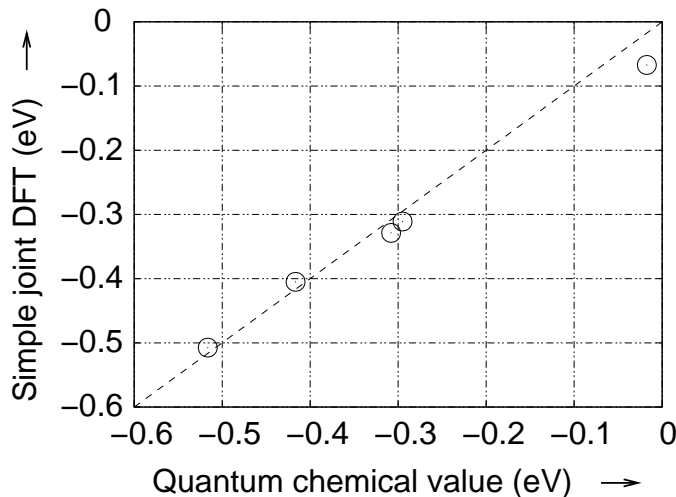


Figure 1. Comparison of predictions of a simple joint density-functional theory (vertical axis) with established quantum chemical values (horizontal axis) for acetamide, acetic acid, methanol, ethanol and methane (from left to right) from [21].

to vacuum behavior. To determine the parameters σ and n_c for this simple model, we fit computed electrostatic solvation energies in aqueous solution ($\epsilon_b = 80$) to the accepted values from the quantum-chemical literature for methane, ethanol, methanol, acetic acid and acetamide[21]. Figure 1 summarizes the quality of this comparison for our final choice of fit parameters, $\sigma = 0.6$ and $n_c = 4.73 \times 10^{-3} \text{ \AA}^{-3}$.

4. RESULTS AND DISCUSSION

4.1. Pristine surface

Ref. [11] reviews in detail the structure of bulk Cr_2O_3 and the relaxation of its pristine (0001) oxygen-terminated surface. Figure 2 shows the relaxed structure of our supercell surface slab. The bulk structure consists of alternating planar layers of oxygen atoms separated by bilayers of chromium. As found in [11], the primary relaxation associated with forming the surface is for the oxygen-terminated surface layers to move inward toward the bulk crystal with slight in-plane displacements.

Figure 3a.1 shows the filled and empty energy levels from our supercell calculation of the (0001) oxygen-terminated surface of Cr_2O_3 in a vacuum environment. Following standard practice, we choose the zero of energy to be the Fermi level, the energy below which states are fully occupied and above which they are empty. The states at the zero line in the figure are thus the highest occupied molecular orbitals (HOMOs) and the first states above the line are the lowest unoccupied molecular orbitals (LUMOs). The figure shows the levels of the pristine surface to be fully filled up to a gap of about 0.5 eV separating the HOMOs and LUMOs.

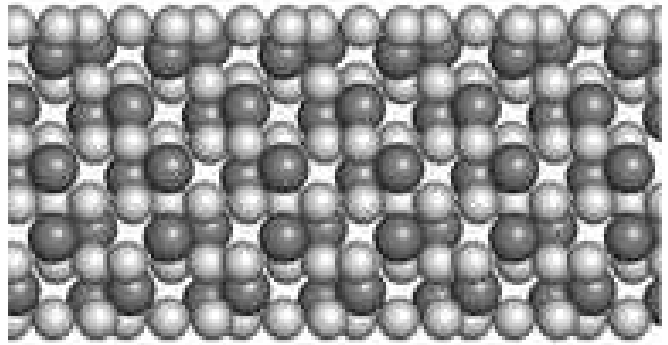


Figure 2. Relaxed structure of pristine surface slab, side view ([0001] direction runs vertically up the page): oxygen (light grey spheres), chromium (dark grey spheres).

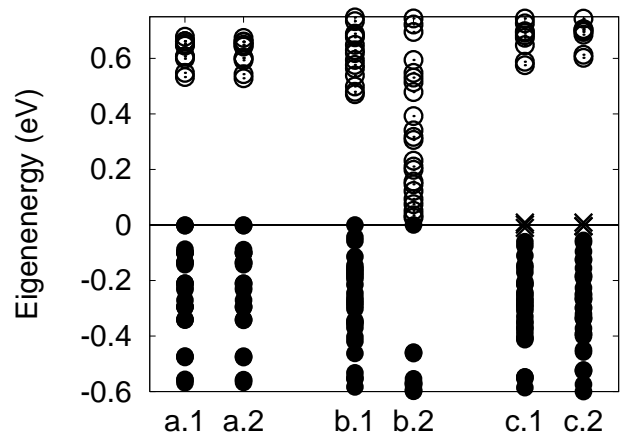


Figure 3. Near-gap energy levels for (a) pristine, (b) hydrogenated and (c) chlorinated system in (1) vacuum and (2) dielectric: filled levels (solid circles), empty levels (open circles), partially filled levels (crosses).

To provide a more global view, Figure 4 presents the density of states, the number of levels from Figure 3a.1 per unit energy as a function of energy, computed using a Gaussian broadening of width $\sigma=0.41$ eV. To underscore the distinction between occupied and unoccupied states, the figure gives a separate curve for each. Finally, as a guide to identification of the bands, the figure also contains markers for the LSDA atomic eigenvalues of oxygen and chromium, which have been shifted uniformly upward by 4.4 eV to approximately counteract the shifting of the Fermi level of the supercell states to zero energy.

Three features in the supercell density of states play important roles in the chemistry of this surface. First, the

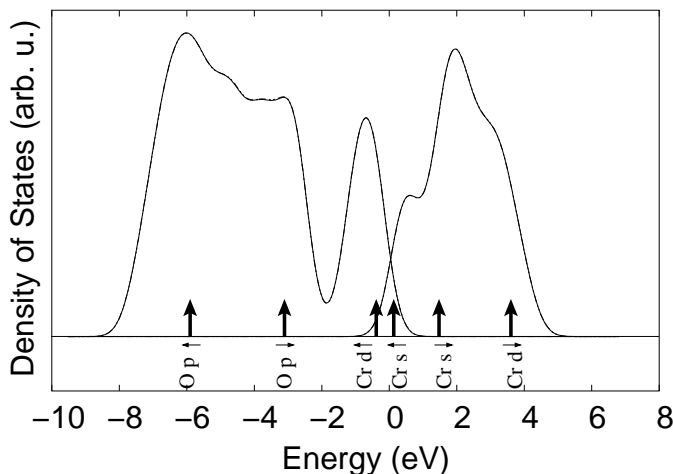


Figure 4. Total density of states of pristine supercell slab in vacuum (solid curve) and in solution (virtually indistinguishable dashed curve): occupied states (curve on left), unoccupied states (curve on right), LSDA atomic eigenvalues (vertical arrows) labeled according to alignment (\uparrow) or anti-alignment (\downarrow) with direction of net atomic spin.

highest occupied *oxygen* orbitals appear as the shoulder (from ~ -4 eV to ~ -2 eV) of the oxygen *2p* band, which consists of “minority” spin electrons, electrons with spin opposite to the net atomic spin. Figure 5a presents the sum of the probabilities associated with states in this range and clearly indicates this shoulder to be a surface oxygen band. The localization of different spin types to either surface corresponds to the fact that the oxygen atoms on each surface have opposite net spin direction. Next, the highest occupied molecular orbitals (HOMOs) overall appear as an *sd*-hybrid chromium band (from ~ -2 eV to ~ 0 eV) consisting of electrons of “majority” spin, spin aligned with the net atomic spin. Figure 6 shows these states to be *bulk* chromium states, with atoms alternating in majority spin direction corresponding to the anti-ferromagnetic nature of the bulk material. Finally, the LUMOs of the system appear as the low energy majority spin shoulder (from ~ 0 eV to ~ 1 eV) of an empty chromium band. Figure 7 shows this shoulder to consist of surface states of primarily chromium character protected under the outer oxygen layer. This character of the HOMOs and LUMOs suggests that any oxygen missing from the outer surface would expose a reactive chromium layer underneath.

Upon repeating the pristine surface calculation in the presence of a dielectric environment, we find virtually no change. There is no change in Figure 2 and, although some very small changes are evident in going from Figure 3a.1 to Figure 3a.2, the global picture of the density of states in Figure 4 is visually indistinguishable for vacuum (solid curve) and dielectric (dashed curve). Finally, inspection of density maps corresponding to Figures 5–7



Figure 5. Contour levels of sum of probability densities from the highest energy shoulder of the oxygen *2p* band, side view ([0001] direction runs vertically up the page): up spin (black surface), down spin (white surface).

again shows no noticeable changes.

4.2. Interaction with hydrogen

Anticipating bonding with oxygen, we initially placed a hydrogen atom in vacuum directly on top of one of the surface oxygen atoms, all of which are equivalent by symmetry. Figure 8a shows that, upon relaxation, the hydrogen atom cants away from the surface perpendicular while appearing to form a bond with the underlying oxygen atom: the final relaxed O-H distance is 0.95 Å, quite close to the experimental O-H separation in H_2O (0.96 Å). Figure 9 shows that the canting of the hydrogen atom is in the same direction as one would expect for the *2p* orbital of the associated oxygen atom given its in-plane displacement. Finally, Figure 10a, which shows the total electron density associated with the chemisorbed H, confirms the presence of the bond as a small protrusion in the density near the hydrogen atom.

Figure 3b.1 shows the filled and empty energy levels of the hydrogenated surface in a vacuum environment. As with the pristine surface (Figure 3a), the energy levels are fully filled up to a HOMO-LUMO gap, consistent with the observed bonding. To better resolve the bond associated with the chemisorbed hydrogen, Figure 11 presents the *local* density of states in the vicinity of the hydrogen atom, which we compute in the same way as the total density of states of Figure 4 but by now weighing each

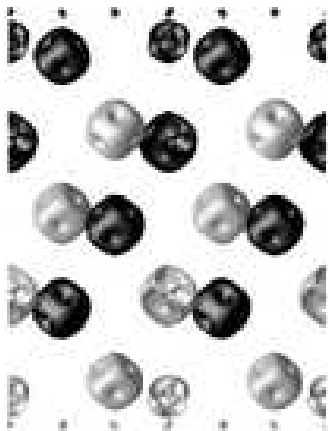


Figure 6. Contour levels of sum of probability densities from the chromium $sd \uparrow$ band, side view ([0001] direction runs vertically up the page): up spin (black surface), down spin (white surface).



Figure 7. Contour level of sum of probability densities from the lowest energy shoulder of the chromium $sd \downarrow$ spin band, side view ([0001] direction runs vertically up the page): up spin (black surface), down spin (white surface).

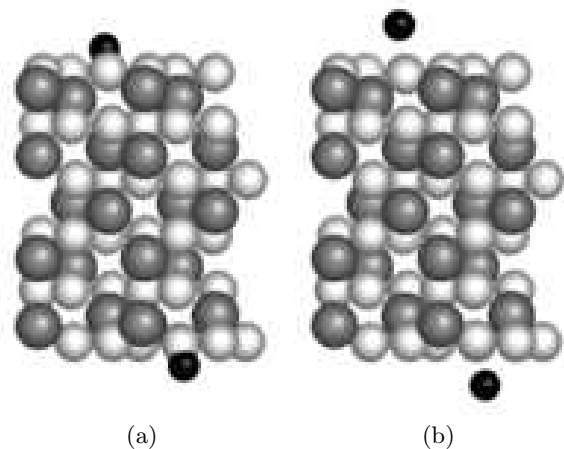


Figure 8. Relaxed structure of surface slab with adsorbed hydrogen in (a) vacuum and (b) dielectric: oxygen (light grey spheres), chromium (dark grey spheres), hydrogen (black spheres). Same view as Figure 2 but showing atoms from a single supercell.

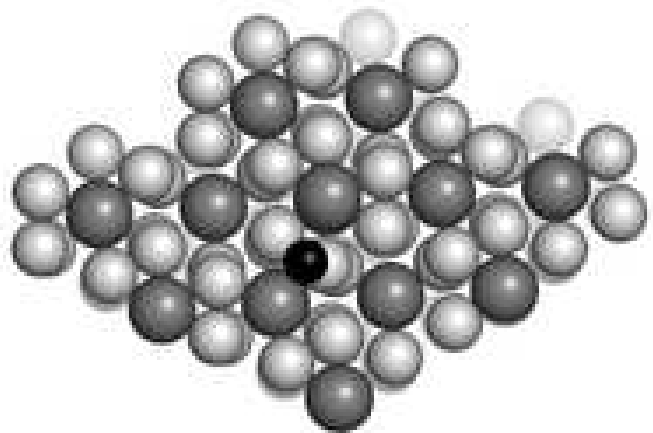
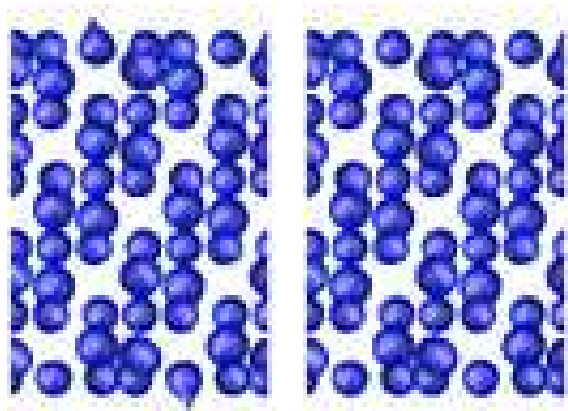


Figure 9. Relaxed structure of single supercell with adsorbed hydrogen in vacuum, top view ([0001] direction normal to page): oxygen (light grey spheres), chromium (dark grey spheres), hydrogen (black sphere).

level with the probability of an electron in the level being within 0.69 \AA of the proton. The local density of states shows that the hydrogen atom interacts mostly with the surface oxygen $2p$ band. A plot of the total density associated with this surface band, Figure 12a, confirms that it contains most of the density protrusion associated with the O-H bond. Finally, Figure 13a shows that the HOMO of the hydrogenated surface, while maintaining significant bulk chromium character, indeed localizes near the hydrogen atom.

To determine the final atomic configuration in the presence of a solvent, we begin with the positions from Figure 8a and relax the atomic coordinates within the ap-



(a)

(a)

Figure 10. Contour level of $0.68 e^-/\text{\AA}^3$ total electron density for hydrogen atom adsorbed on oxygen-terminated (0001) surface in (a) vacuum and (b) dielectric, side view ([0001] direction runs vertically up the page).

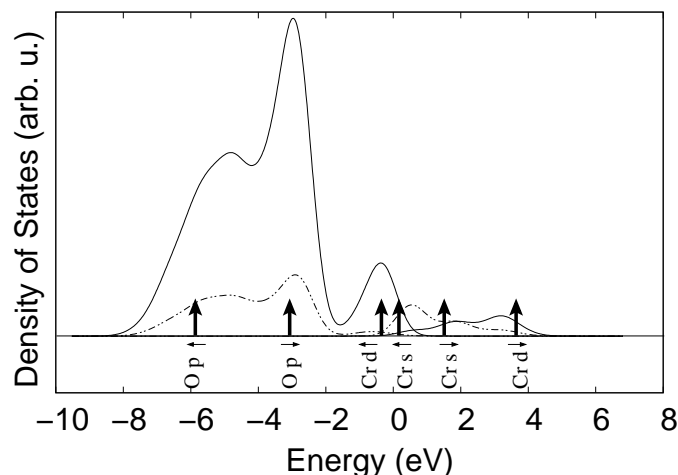


Figure 11. Local density of states within 0.69 \AA of the proton for hydrogen interacting with oxygen-terminated (0001) surface in vacuum (solid curve) and solution (dashed curve). Same conventions as Figure 4.

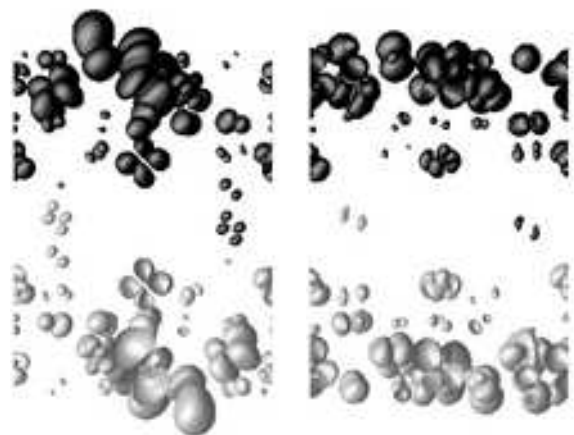
proximate joint density functional (3,4) until the maximum force on any atom is less than 0.3 eV/\AA . Figure 8b, which displays the resulting configuration, shows that the presence of the dielectric has a dramatic effect on the hydrogen. The nearest oxygen-hydrogen distance has increased to 2.3 \AA , clearly breaking the O-H bond and returning the hydrogen atom to the solution. Consistent with this picture, the largest residual force remains on the hydrogen atom in the direction tending to push it



(a)

(b)

Figure 12. Contour level of sum of probability densities associated with oxygen $2p$ surface band in (a) vacuum and (b) dielectric: up spin (black surface), down spin (white surface).



(a)

(b)

Figure 13. Contour level of HOMO of hydrogen interacting with the oxygen-terminated (0001) surface in (a) vacuum and (b) dielectric, side view ([0001] direction runs vertically up the page): up spin (black surface), down spin (white surface).

yet further from the surface. Lack of any indication of the presence of the hydrogen atom in the resulting total charge density, Figure 10b, indicates that the atom enters the solution as an ion.

Figure 3b.2 shows that upon the removal of the proton from the surface, the excess electron from the O-H bond appears simply as a donated conduction electron

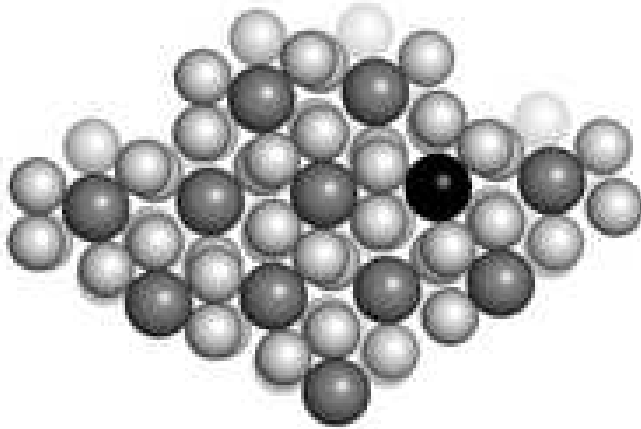


Figure 14. Relaxed structure of surface interacting with chlorine in vacuum: oxygen (light grey spheres), chromium (dark grey spheres), chlorine (black sphere): top view ([0001] direction perpendicular to page).

just above the energy gap. Consistent with this donation, the dashed curve in Figure 11 shows a dramatic reduction in the local density of states near the proton, and the HOMO in Figure 13b now shows more of the surface chromium character of the original LUMO band from Figure 7.

4.3. Interaction with chlorine

Anticipating the possibilities of ionic bonding for chlorine, we initially placed (in the 1×1 surface supercell) a chlorine atom in vacuum directly above each of the two distinct types of Cr^{3+} site from the outermost chromium bilayer and found the site above the innermost of the two component layers to be favored by 0.4 eV. Figure 14 shows a top ([0001]) view of the relaxed configuration for this site when computed within the 4×4 supercell. We find relatively little relaxation from the clean surface structure (movement of all surface atoms is less than 0.01 Å) with the chlorine ion settling upon relaxation to a position with a chlorine-oxygen separation of 2.6 Å, only 20% smaller than the sum of the nominal ionic radii, 3.1 Å. Figure 15a shows a side view of the total electron density for a surface with adsorbed Cl in vacuum, illustrating the physisorbed nature of the interaction.

Turning to the energy levels, Figure 3c.1 shows the levels near the gap. In this case, three two-thirds filled states (degenerate to within 19 meV \sim 220 K) appear just below the top of the gap, indicating the presence of a hole in the Cr band, which we interpret as arising from the chlorine atom absorbing an electron from the chromium oxide to become Cl^- . To explore local effects from the adsorbed chlorine, Figure 16 presents the local density of states, weighing each state with the probability of an electron being within 1.6 Å of the chlorine nucleus. In

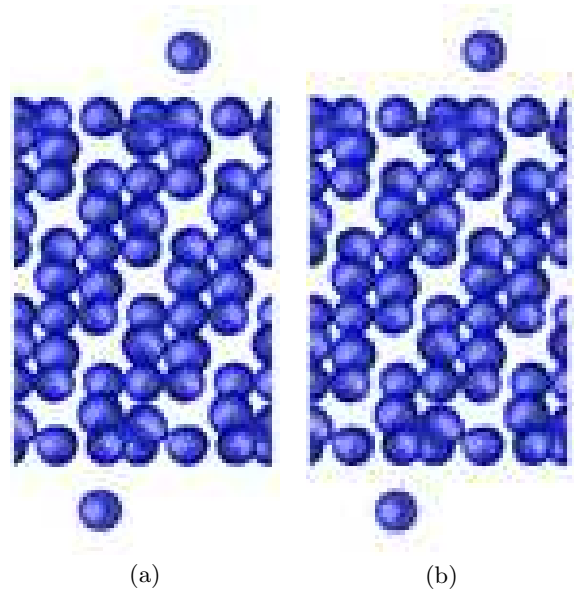


Figure 15. Contour level of $0.68 \text{ e}^-/\text{\AA}^3$ total electron density for chlorine atom adsorbed on oxygen-terminated (0001) surface in (a) vacuum and (b) dielectric, side view ([0001] direction runs vertically up the page).

contrast to the local density of states of the hydrogen calculation, the appearance of the oxygen band is significantly reduced and there is much stronger mixing with the bulk chromium states. This mixing corresponds to alignment of the barely bound Cl^- states with the bulk HOMO chromium band as the chlorine ion draws electrons from the bulk chromium band, which is serving as a reservoir of electrons. Finally, Figure 17a shows the sum of the electron probabilities in the partially filled states at the Fermi level, which are thus both the HOMOs and the LUMOs. Interpreted as the sum states lacking exactly one electron from full occupancy, the figure shows the spatial distribution of the hole which the formation of the Cl^- injects into the chromium-oxide slab. As one would expect, this (positive) hole tends to localize to the vicinity of the Cl^- ions.

Upon relaxation of the physisorbed chlorine surface in the presence of the solvent, we find there to be very little relaxation (no more than 0.01 Å for any atom), little difference in the total charge density (Figure 15b), no change in the presence of partially filled states at the Fermi level (Figure 3c.2), and very little difference in the local density of states (Figure 16) or the spatial distribution of the hole injected into surface, Figure 17b.

4.4. Conclusions

Above, we introduce the novel approach of using a joint density-functional theory to treat an *ab initio* electronic structure calculation in the presence of a liquid solvent such as water. The resulting approach is the first practi-

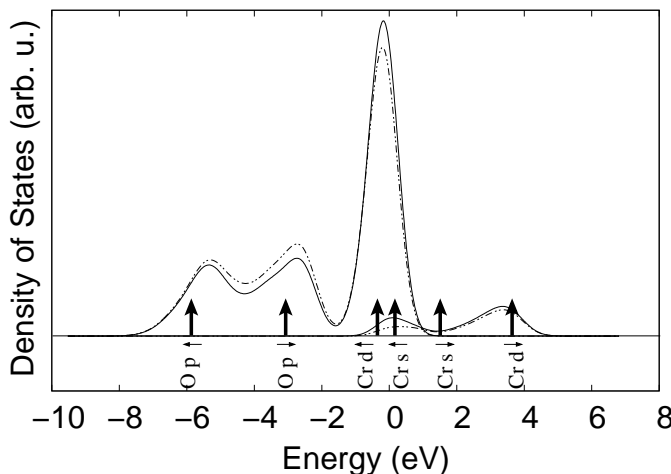


Figure 16. Local density of states within 1.6 Å of the chlorine nucleus for chlorine interacting with oxygen-terminated (0001) surface in vacuum (solid curve) and solution (dashed curve). Same conventions as Figure 4.

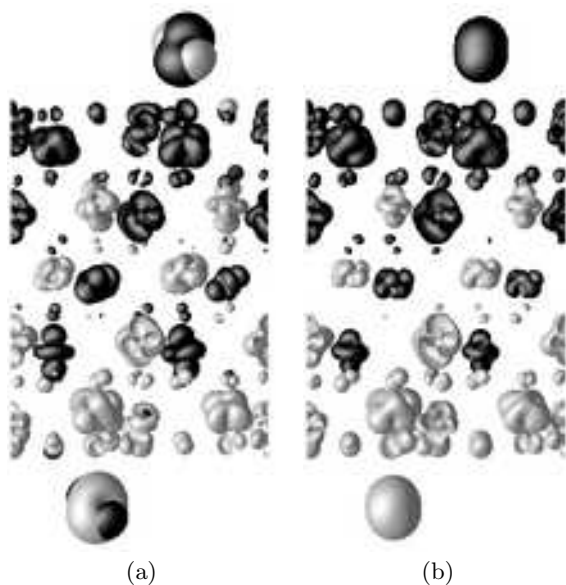


Figure 17. Contour level of HOMOs and LUMOs (equivalent in this case) of chlorine interaction with oxygen-terminated (0001) surface in (a) vacuum and (b) dielectric, side view ([0001] directions runs vertically up the page).

cal *ab initio* approach for the treatment of the interaction of complex surfaces with chemical species in the presence of a dielectric environment.

Through this approach, we find the mode of interaction of the oxygen-terminated Cr_2O_3 (0001) surface with hydrogen to be covalent bonding while that with chlorine to be ionic bonding. The presence of a dielectric solvent has very little effect on the pristine surface or on its inter-

action with chlorine, while it has a dramatic effect on the interaction with hydrogen. In vacuum, hydrogen readily forms an O-H bond with the outermost layer of atoms of the surface. In the presence of water, the strong screening associated with dielectric effects in the vicinity of the proton (ultimately via hydrogen bonding interactions) so weakens the attractive potential of the proton that the covalent bond is broken, the electron is released into the surface and the proton solvates.

In contrast, the interaction with chlorine in vacuum is already ionic, with a neutral chlorine atom having sufficient electronegativity to draw an electron from the bulk of the crystal and thus ionize to Cl^- while injecting a hole into the bulk. The presence of a dielectric solvent tends to screen the excess charge on the chlorine ion, thereby only further stabilizing this form of interaction with the surface so that there is little change in this case when going from vacuum to a dielectric environment. It thus appears that the primary reason why the solvent has a much greater effect on the interaction with hydrogen than with chlorine is that a dielectric environment generally favors the formation of ions and the surface interaction with chlorine is already ionic whereas the interaction with hydrogen in vacuum is covalent.

We believe that there would be little effect on these conclusions were the calculations to be performed with ions rather than atoms. Doing so would involve principally removing a single electron from the calculation for each hydrogen atom or adding an electron for each chlorine atom. For the chlorine cases, this would simply remove the relatively delocalized hole from the bulk chromium band and thus likely have little effect on the final results. For the interaction with hydrogen, the removal of an electron would, in the dielectric case, simply remove the relatively delocalized donated electron or, in the vacuum case, likely simply introduce a relatively delocalized hole into the chromium band. In either of these cases for hydrogen, we again would expect little disruption of the chemical integrity of the surface.

Overall, a novel picture emerges to explain how the oxygen-terminated surface of Cr_2O_3 is particularly protective in a hydrochloric acid solution. The outer oxygen layer provides a natural barrier to interaction with chlorine but might be expected to interact strongly with protons. However, through dielectric screening effects, it is the aqueous environment itself which eliminates the outer oxygen layer's natural tendency to interact with hydrogen.

These first calculations of surface chemistry in the presence of a solvent make clear the need for additional work to complete the picture of the passivating effects of chromium oxide. We would next like to study the interaction of chlorine and hydrogen with a *chromium*-terminated surface, whose HOMOs would then be exposed on the surface rather than protected under the outer oxygen layer. We also would like to explore pit corrosion by calculating the interaction of the aforementioned species with a step in the passivating oxygen layer.

Finally, we would like to contrast the interactions of chlorine in such systems to the interactions of fluorine and bromine in order to better understand the corrosive success of chlorine relative to these other species.

5. ACKNOWLEDGMENTS

This work was funded by NSF GRANT #CHE-0113670. AAR would like to thank Jefferson W. Tester and Ronald M. Latanision for planting the seed of this project during her 1994–1995 sabbatic leave at MIT.

References and Notes

- [1] Radeke, M.; Carter, E. *Annu. Rev. Phys. Chem.* **1997**, *48*, 243–270.
- [2] Greeley, J.; Norskov, J.; Mavrikakis, M. *Annu. Rev. Phys. Chem.* **2002**, *53*, 319–348.
- [3] Gross, A. *Surface Science* **2002**, *500*, 139–147.
- [4] DeGaspari, J. *Mechanical Engineering* **2003**, *125*, 30.
- [5] Ryan, M.; Chater, D. W. R.; Hutton, B.; McPhail, D. *Nature* **2002**, *415*, 770–774.
- [6] Stampfl, C.; Ganduglia-Pirovano, M.; Reuter, K.; Scheffler, M. *Surface Science* **2002**, *500*, 368–394.
- [7] Erlebacher, J.; Aziz, M.; Karma, A.; Dimitov, N.; Sieradzki, K. *Nature* **2001**, *410*, 450–453.
- [8] Jones, P. *Principles and Prevention of Corrosion*; Prentice Hall: Upper Saddle River, NJ, 1996.
- [9] Latanision, R.; Mitton, D.; Zhang, S.; Cline, J.; Caputy, N.; Arias, T. In *Fourth International Symposium on Supercritical Fluids*, Vol. C, pages 865–868, Sendai, Japan, 1997.
- [10] Alavi, S.; Sorescu, D. C.; Thompson, D. L. *J. Phys. Chem. B* **2003**, *107*, 186.
- [11] Cline, J. A.; Rigos, A. A.; Arias, T. A. *The Journal of Chemical Chemistry B* **2000**, *104*, 6195–6201.
- [12] Tannor, D.; Marten, B.; Murphy, R.; Friesner, R.; Sitkoff, D.; Nicholls, A.; Ringnalda, M.; III, W. G.; Honig, B. *J. Am. Chem. Soc.* **1994**, *116*, 11875–11882.
- [13] Fattebert, J.-L.; Gygi, F. *J. Comput. Chem.* **2002**, *23*, 662–666.
- [14] Payne, M.; Teter, M.; Allan, D.; Arias, T.; Joannopoulos, J. *Reviews of Modern Physics* **1992**, *64*, 1045.
- [15] Curtin, W.; Ashcroft, N. W. *Phys. Rev. A* **1985**, *32*, 2909.
- [16] Sun, S. X. *Phys. Rev. E* **2001**, *64*, 021512.
- [17] Petrosyan, A.; Arias, T. A. *Phys. Rev. Lett.* **not published yet**.
- [18] Perdew, J. P.; Wang, Y. *Phys. Rev. B* **1992**, *45*, 13244.
- [19] Kleinman, L.; Bylander, D. M. *Phys. Rev. Lett.* **1982**, *4*, 1425.
- [20] Arias, T. A.; Payne, M. C.; Joannopoulos, J. D. *Phys. Rev. Lett.* **1992**, *69*, 1077.
- [21] Marten, B.; Kim, K.; Cortis, C.; Friesner, R. A.; Murphy, R. B.; Ringnalda, M. N.; Sitkoff, D.; Honig, B. *J. Phys. Chem.* **1996**, *100*, 11775.